Available online at www.sciencedirect.com
SCIENCE DIRECT®
Journal of Theoretical Biology 229 (2004) 293–309
Journal of Theoretical Biology
www.elsevier.com/locate/jtbi

Modeling the interactions between osteoblast and osteoclast activities in bone remodeling

Vincent Lemaire[a,*], Frank L. Tobin[a,1], Larry D. Greller[a,2], Carolyn R. Cho[a,3], Larry J. Suva[b,4]

[a] *Scientific Computing and Mathematical Modeling, GlaxoSmithKline, King of Prussia, PA, USA*
[b] *Bone & Cartilage Biology, GlaxoSmithKline, King of Prussia, PA, USA*

Received 23 April 2003; received in revised form 27 January 2004; accepted 29 March 2004

Abstract

We propose a mathematical model explaining the interactions between osteoblasts and osteoclasts, two cell types specialized in the maintenance of the bone integrity. Bone is a dynamic, living tissue whose structure and shape continuously evolves during life. It has the ability to change architecture by removal of old bone and replacement with newly formed bone in a localized process called remodeling. The model described here is based on the idea that the relative proportions of immature and mature osteoblasts control the degree of osteoclastic activity. In addition, osteoclasts control osteoblasts differentially depending on their stage of differentiation. Despite the tremendous complexity of the bone regulatory system and its fragmentary understanding, we obtain surprisingly good correlations between the model simulations and the experimental observations extracted from the literature. The model results corroborate all behaviors of the bone remodeling system that we have simulated, including the tight coupling between osteoblasts and osteoclasts, the catabolic effect induced by continuous administration of PTH, the catabolic action of RANKL, as well as its reversal by soluble antagonist OPG. The model is also able to simulate metabolic bone diseases such as estrogen deficiency, vitamin D deficiency, senescence and glucocorticoid excess. Conversely, possible routes for therapeutic interventions are tested and evaluated. Our model confirms that anti-resorptive therapies are unable to partially restore bone loss, whereas bone formation therapies yield better results. The model enables us to determine and evaluate potential therapies based on their efficacy. In particular, the model predicts that combinations of anti-resorptive and anabolic therapies provide significant benefits compared with monotherapy, especially for certain type of skeletal disease. Finally, the model clearly indicates that increasing the size of the pool of preosteoblasts is an essential ingredient for the therapeutic manipulation of bone formation. This model was conceived as the first step in a bone turnover modeling platform. These initial modeling results are extremely encouraging and lead us to proceed with additional explorations into bone turnover and skeletal remodeling.

Keywords: Mathematical modeling; Bone cells; Osteoporosis; Therapeutic strategies; Differentiation; Parathyroid hormone

1. Introduction

Bone is a dynamic, living tissue whose structure and shape continuously adjusts to mainly provide structural framework. A rigid skeleton makes it possible to support weight and ensures protection for the muscles and organs. In addition, bone is the primary site of hematopoiesis. Bone also participates in the maintenance of serum-mineral metabolism, and is considered an important component of the immune system.

The fabric of bone is a unique composite of living cells embedded in a remarkable three-dimensional

*Corresponding author. Present address: Department of Physiology, Centre for Nonlinear Dynamics in Physiology and Medicine, McGill University, 3655 Prom. Sir William Osler, Montreal, QC, Canada.Tel.: +514-398-8092; fax: +514-398-745.
E-mail addresses: lemaire@cnd.mcgill.ca (V. Lemaire), frank_tobin@gsk.com (F.L. Tobin).
[1] Also for correspondence.
[2] Present address: Biosystemix, Ltd., Syolenham, ON, Canada.
[3] Present address: Predix Pharmaceuticals, Woburn, MA, USA.
[4] Present address: Center for Orthopedic Research, University of Arkansas for Medical Sciences, Little Rock, AR, USA.

0022-5193/$ - see front matter © 2004 Elsevier Ltd. All rights reserved.
doi:10.1016/j.jtbi.2004.03.023

mineralized structure resembling a honeycomb. Cancellous bone consists of a highly connected network of vertical and horizontal struts, called trabeculae. Most trabeculae are oriented along force-field lines of recurrent mechanical stress, while the remainder strengthen the network by joining perpendicularly to adjacent trabeculae. Even after developmental and longitudinal growth of the skeleton is complete, bone retains its ability to change its internal structure by removal of old bone and its replacement with newly formed bone in localized processes called remodeling. Remodeling is a fundamental property of bone that permits adaptation to a changing mechanical environment. Packets of bone are removed where the mechanical demand of the skeleton is low and new bone is formed at those sites where mechanical strains are repeatedly detected.

Remodeling also permits the restoration of microdamage caused by fatigue and shock. This constant care of the bone matrix prevents its premature deterioration and maintains its overall strength. Remodeling is a complex process performed by the coordinated activities of osteoblasts and osteoclasts. Osteoblasts are of mesenchymal origin and are the cells responsible for the synthesis of the bone matrix. Osteoclasts are hematopoietic in origin and are the only cells capable of resorbing mineralized bone. The interactions between osteoblasts and osteoclasts, which guarantee a proper balance between bone gain and loss, is known as coupling (Rodan and Martin, 1981). Metabolic bone diseases appear when a biochemical or cellular link of this finely organized network is chronically disrupted.

Our research motivation is to develop a theoretical framework that may explain experimental observations in bone biology. In particular, we are interested in exploring failures of the biochemical control network that lead to bone diseases such as osteoporosis. In the present paper, we propose a mathematical model of the cellular control of bone remodeling to examine these issues. In particular, we have developed a synthetic system which includes the main cellular and biochemical feedbacks mechanisms responsible for the regulation of bone turnover.

There have been few attempts to mathematically define the dynamics of bone remodeling at the cellular level. We are aware of only three such papers. Two of them propose a mathematical model accounting for the differential activity of PTH administration on bone accumulation (Kroll, 2000; Rattanakul et al., 2003). The third paper proposes a mathematical model of autocrine and paracrine interactions among osteoblasts and osteoclasts (Komarova et al., 2003). Our model is the first to incorporate the RANK-RANKL-OPG pathway, which is widely considered essential for the regulation of osteoclast formation.

Using our model, it is possible to simulate skeletal disease by inserting dysfunctional connections in the coupling network to explore different disease hypotheses. Conversely, potential routes for putative therapeutic intervention have been determined.

2. Model development

Bone remodeling is largely a localized phenomenon, likely under the control of local factors (Mundy et al., 1996). However, it is clear that systemic hormones also modulate the effects on various local factors, and consequently the rate of bone remodeling. For example, estrogen promotes osteoclast apoptosis that seems to be mediated by local factors such as transforming growth factor beta (TGF-β) (Boyce et al., 1999). This type of local regulation provides tonic baseline control, upon which hormonal inputs (as well as mechanical) operate (Manolagas, 2000). One of the modeling issues to address is to consider whether the pathogenesis of cancellous bone loss (such as in osteoporosis) is related to the failure of local regulation, rather than a systemic disorder. A list of biological assumptions and supporting observations upon which the model is based are presented in the appendix.

2.1. Structure of the core model

The logical structure of the model is presented in Fig. 1. The schematic presents the simplified lineages of osteoblasts, osteoclasts and their interactions. The basis for the selection of this specific structure is based on our understanding of bone turnover and remodeling.

During osteoblastic differentiation, seven stages of cell maturation and differentiation have been characterized: from mesenchymal stem cells to osteocyte and lining cells (Aubin, 1998a). Our model accounts for four of the major differentiation stages (two of them being actual state variables in the model), representing osteoblastic primary functions namely, coupling, bone formation, response to hormonal inputs.

The source of the osteoblastic lineage is a large reservoir of uncommitted mesenchymal progenitors capable of differentiating into osteoblastic cells (as well as into other types of cells such as myocytes and adipocytes) (Aubin, 1998b). Once they commit to the osteoblastic lineage, the progenitors differentiate into "responding osteoblasts" (ROB). This category is not considered a "true" cell type, but rather a composite of several phenotypes that share similar characteristics. They are both early osteoblasts or preosteoblasts and are highly responsive to differentiation signals (Aubin, 1998b). These cells are persuaded to differentiate further under the complex effects of specific factors such as PTH and TGF-β (Aubin, 1998b). This latter

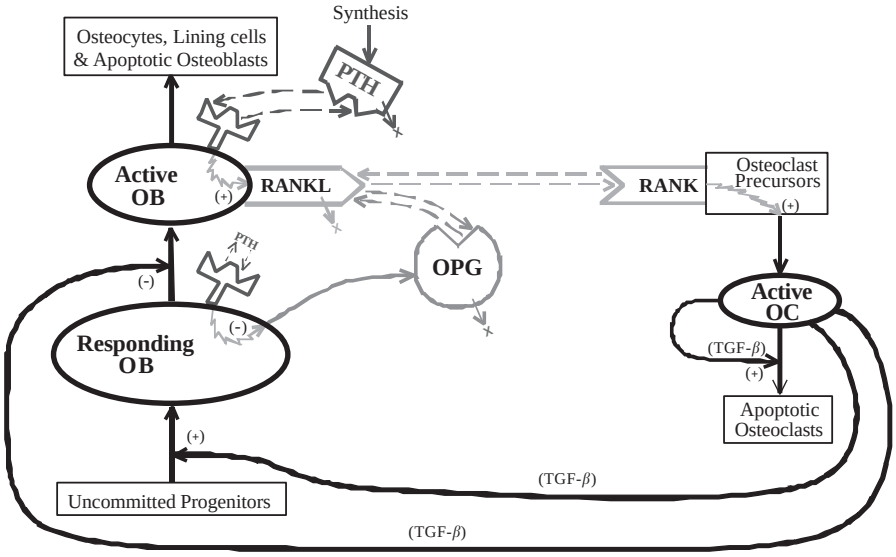

Fig. 1. Diagrammatic representation of the basic structure of the model. The ovals represent cell compartments. The solid arrows represent flows of the pointed element. The solid arrows with a (+) (or (−) sign) next to them indicate a stimulatory (or inhibitory) action. The zigzag arrows represent cellular signaling pathways leading to an increasing (or a diminishing) production of the indicated agent. The small arrows pointing at an 'X' indicate an elimination flow. The double dashed arrows represent receptor/ligand binding. The thin squared frames indicate types of cells which are not included in the model.

characteristic contributes, in part, to the creation of a reservoir of potentially active osteoblasts and is a fundamental phenomenon in the control of bone remodeling (Mundy, 1999).

The maintenance of this reservoir is under strict control of the osteoclast (Mundy, 1999). After further differentiation, responding osteoblasts mature to active osteoblasts (AOB), which, in turn, are responsible for bone formation. Eventually, osteoblasts either die or transform to either lining cells or osteocytes (Jilka et al., 1998). In the model there is no feedback movement from lining cells to osteoblasts, so once cells have left the active osteoblast compartment they are presumably no longer capable of active bone formation.

The osteoclast lineage is also complex, but perhaps better defined — consisting of at least four different types of cells, beginning with the hematopoietic precursor and culminating in the apoptotic, differentiated osteoclast (Roodman, 1999; Teitelbaum, 2000). In the model, only three types of osteoclasts are considered, one being an actual state variable. Precursors differentiate to active osteoclasts (AOC), which resorb bone at a rate proportional to their number. Apoptosis is the ultimate stage at the end of the lineage.

Committed stromal cells of osteoblastic lineage stimulate, through cell-to-cell contact, the differentiation of osteoclastic progenitors and their fusion into multinucleated active osteoclasts (Martin and Ng, 1994). The agents supporting cell contact are the receptor activator of NF-κB (RANK), a membrane-bound cytokine-like molecule expressed in hematopoietic osteoclastic progenitors (Aubin and Bonnelye, 2000), and RANK ligand (RANKL), a TNF-related transmembrane cytokine expressed by committed preosteoblastic cell (Burgess et al., 1999). RANKL is expressed on the surface of osteoblastic cells and bone marrow stromal cells (Collin-Osdoby et al., 2001), and binds to the RANK receptor, present on the surface of osteoclastic precursors, thereby stimulating the differentiation and activation of osteoclasts (Burgess et al., 1999; Aubin and Bonnelye, 2000; Hofbauer et al., 2000). RANKL action is negatively regulated by osteoprotegerin (OPG), a soluble receptor sequestering RANKL and thus antagonizing binding to RANK (Filvaroff and Derynck, 1998; Greenfield et al., 1999; Gunther and Schinke, 2000). OPG is produced and released by osteoblasts (Filvaroff and Derynck, 1998; Aubin and Bonnelye, 2000; Hofbauer et al., 2000).

Bone matrix is the largest source of TGF-β in the body (Roodman, 1999). Indeed, the content of TGF-β in dried bone powder is approximately 1000-fold greater than the levels required for osteoblastic stimulation (Hauschka, 1989). TGF-β, as well as other growth factors and specific components embedded in the bone matrix, are released by osteoclasts during bone resorption (Bonewald and Dallas, 1994). TGF-β's effect on osteoblasts is bi-directional depending upon the state of maturation of the osteoblasts (Hauschka, 1989; Simmons and Grynpas, 1990). On one hand, TGF-β has the potential to stimulate osteoblast recruitment, migration and proliferation of osteoblast precursors (meaning ROBs in our case) (Eriksen and Kassem, 1992; Bonewald and Dallas, 1994; Mundy et al., 1996). On the other, TGF-β inhibits terminal osteoblastic

differentiation into AOBs (Alliston et al., 2001). Thus, the number of ROBs increases under the influence of TGF-β. When TGF-β is removed or becomes inactivated, the increased pool of ROBs undergoes differentiation, thus increasing the number of AOBs (Mundy, 1999). The inhibitory effect of TGF-β is mediated by core binding factor a1 (Cbfa1), which is a potent osteoblast differentiation factor (Ducy et al., 2000; Alliston et al., 2001). TGF-β is also known to induce osteoclast apoptosis (Greenfield et al., 1999; Roodman, 1999).

The RANK-RANKL-OPG pathway, coupled to the dual action of TGF-β on osteoblasts, constitutes a basic control network, capable of regulating bone remodeling, and is the core of this model. The molecular and cellular interactions generated by this complex network create the necessary dynamics responsible for maintaining the tight coupling observed between osteoblasts and osteoclasts during normal bone turnover. While many simplifying assumptions have been made in identifying this core behavior (Appendix), it permits a detailed focus on the intrinsic mechanisms to be explained.

2.2. Hormonal inputs

Several systemic hormones, such as glucocorticoids, estrogen, PTH and vitamin D, have multiple effects on bone cell proliferation, differentiation, activation, and apoptosis rates (Huang and Zheng, 1999; Bland, 2000). The choice to include PTH in the model is not arbitrary, since PTH (in concert with vitamin D) is the most important hormone regulating calcium homeostasis and bone remodeling (Parfitt, 1976). Moreover, PTH is currently involved in numerous clinical trials as an anabolic agent for the treatment of low bone mass in osteoporosis (Jerome et al., 2001; Neer et al., 2001; Seeman and Delmas, 2001), and Forteo (PTH 1-34) was recently approved by the Food and Drug Administration (Neer et al., 2001; Whitfield et al., 2002).

PTH has catabolic effects on bone when released into the plasma quasi-continuously or continuously, causing the calcium level to raise in the blood circulation (Watson et al., 1999). Yet, PTH is also a potent anabolic agent when injected on a pulsatory schedule (Dempster et al., 1993; Meng et al., 1996). Although Kroll provided an alternate explanation for the anabolic response to pulsatile PTH based on delayed interactions between osteoblasts and osteoclasts (Kroll, 2000), it is believed that the anabolic action of PTH is induced by differential osteoblastic signaling kinetics, presumably transduced through PTH binding to its receptor on the osteoblast surface (Lowik et al., 1985; Fujimori et al., 1991; Dempster et al., 1993; Cho et al., 2000). Our model is not designed to describe the anabolic response of the skeleton to pulsatile PTH administration, but rather it incorporates the role of PTH in normal bone and calcium homeostasis.

PTH receptors are largely expressed on the osteoblast surface (Goltzman, 1999; Teitelbaum, 2000). Quasi-steady state levels of plasma PTH, by binding these receptors, stimulates the production of RANKL and inhibits the production of OPG by osteoblasts (Aubin and Bonnelye, 2000; Teitelbaum, 2000; Halladay et al., 2001; Ma et al., 2001), which causes an increase in AOC numbers. Direct effects of PTH on osteoblasts have also been experimentally observed (Isogai et al., 1996; Goltzman, 1999; Du et al., 2000). In the model, the PTH-induced osteoblast-to-osteoclast signaling effects are mediated solely through the RANK-RANKL-OPG pathway.

2.3. Mathematical formulation

In the model (Fig. 1), cellular interactions are carried out via activation of cell receptors. The receptors either bind molecules secreted by other cell types (endocrine and paracrine modes), or with molecules secreted by the same cell (autocrine mode), or with other transmembrane molecules via direct cell-to-cell contacts. The different cell types represented in the model respond to the activation of their receptors by producing new molecules, differentiating, or dying. The mathematical formulation of the model is primarily influenced by physiological events involving receptor binding and intracellular signaling modeling (Knauer et al., 1984; Lauffenburger and Linderman, 1996).

Without considering the osteoblastic interactions, the reaction scheme of the binding of PTH with its receptor is represented as follows:

$$\begin{array}{c} {\scriptstyle p_P}\\ \downarrow\\ P \\ \downarrow\\ {\scriptstyle d_P} \end{array} + P_r \underset{k_6}{\overset{k_5}{\rightleftharpoons}} P_r \bullet P, \tag{1}$$

where p_P and d_P are abbreviations for PTH production and destruction fluxes, respectively. $P_r \bullet P$ is the complex formed by PTH and its receptor. We suppose that the law of mass action applies to reaction (1), as described by the following ordinary differential equations (Lauffenburger and Linderman, 1996), where we have included the effects of the two osteoblast locations where PTH binding occurs (see Fig. 1):

$$\frac{\mathrm{d}P}{\mathrm{d}t} = S_P + I_P + \left(k_6 \cdot P_r \bullet P - k_5\left(R_T^P - P_r \bullet P\right) \cdot P\right) \cdot (B + R) - k_P \cdot P,$$

$$\frac{\mathrm{d}P_r \bullet P}{\mathrm{d}t} = k_5\left(R_T^P - P_r \bullet P\right) \cdot P - k_6 \cdot P_r \bullet P,$$

where $S_P + I_P$ is the overall PTH production and k_P a first-order degradation rate. S_P represents the basal synthesis rate of PTH (supposed to be fixed), and I_P is the external rate of PTH injection. Depending on the

profile of administration, I_P may be constant or may depend on time. R_T^P is the number of PTH receptors per cell. This number is supposed to be constant, implying that no significant synthesis, degradation, internalization, or recycling of receptors occurs over the time frame for which the model applies. B and R are the concentrations of, respectively, the AOBs and ROBs. The PTH binding reaction (1) equilibrates much more rapidly than the time it takes for the cell populations of the model to change noticeably. It is also the case for all other binding reaction of the model. Consequently, only the steady states of these molecular events really alter the cell dynamics in the model. At equilibrium, the proportion of occupied PTH receptors is given by $\pi_P = P_r \bullet P/R_T^P = P/(P+P^s)$, where $P^s = k_6/k_5$, whereas the PTH concentration is $P = (S_P + I_P)/k_P = P^0 + \bar{P}$, with $P^0 = S_P/k_P$ and $\bar{P} = I_P/k_P$. Thus, we have

$$\pi_p = \frac{P}{P+P^s} \approx \frac{\bar{P}+P^0}{\bar{P}+P^s} \tag{2}$$

for $P^0 \ll P^s$.

The reactions schemes of the bindings of OPG (O) with RANKL (L) and RANKL with RANK (K) are the following:

$$\begin{array}{ccc} {\scriptstyle p_0}\downarrow & {\scriptstyle p_L}\downarrow & \\ O & + L & \underset{k_2}{\overset{k_1}{\rightleftharpoons}} O\bullet L \\ \downarrow {\scriptstyle d_0} & \downarrow {\scriptstyle d_L} & \end{array} \quad \text{and} \quad \begin{array}{ccc} & {\scriptstyle p_L}\downarrow & \\ L & + K & \underset{k_4}{\overset{k_3}{\rightleftharpoons}} K\bullet L \\ \downarrow {\scriptstyle d_L} & & \end{array}$$

$O\bullet L$ and $K\bullet L$ represent, respectively, the OPG-RANKL and RANK-RANKL complexes. The differential equations describing the time evolution of the variables O, L, $O\bullet L$ and $K\bullet L$ (K is not considered as a model variable, the concentration of RANK is kept fixed to reflect the undiminished availability of the osteoclast precursors) are the following (Lauffenburger and Linderman, 1996):

$$\begin{aligned} \frac{\mathrm{d}O}{\mathrm{d}t} &= p_O - k_1 \cdot O \cdot L + k_2 \cdot O\bullet L - d_O, \\ \frac{\mathrm{d}O\bullet L}{\mathrm{d}t} &= k_1 \cdot O \cdot L - k_2 \cdot O\bullet L, \\ \frac{\mathrm{d}L}{\mathrm{d}t} &= p_L - k_1 \cdot O \cdot L + k_2 \cdot O\bullet L - k_3 \cdot K \cdot L \\ &\quad + k_4 \cdot K\bullet L - d_L, \\ \frac{\mathrm{d}K\bullet L}{\mathrm{d}t} &= k_3 \cdot K \cdot L - k_4 \cdot K\bullet L, \end{aligned} \tag{3}$$

d_O is a linear degradation function: $d_O = k_O \cdot O$.

The production of the receptor-mediated cell behavioral response is a function of the receptor occupancy. A model, offered by (Knauer et al., 1984), relates the cell proliferation rate to growth factor binding. In this paper, the authors propose that the cell proliferation rate is proportional to the receptor occupancy. We postulate, at least to first order, that the linear relationship between the cell response and the receptor occupancy is applicable to other types of cell responses (not just cell proliferation). Consequently, in our model, and in the case of a "proliferative" cell response, the cell response is proportional to receptor occupancy. Whereas, "anti-proliferative" cell responses are inversely proportional to the receptor occupancy. Thus, as the production rate of OPG is down-regulated by PTH, it is represented by an inversely proportional relation with the PTH receptor occupancy fraction

$$p_O = \frac{K_O^P}{\pi_P} R + I_O, \tag{4}$$

where K_O^P is the minimal production rate of OPG per cell, π_P is the proportion of occupied PTH receptors given in (2), and I_O is a rate of external injection of OPG.

Unlike OPG, RANKL, is attached to osteoblast surfaces and occupies a restricted space. The surface of osteoblasts may only carry a limited number of RANKL molecules. Therefore, the RANKL production rate p_L should be self-limited to prevent the number of RANKL from exceeding the carrying capacity of the osteoblast surface. The effective carrying capacity is imposed by the cell response to PTH binding, although there is an absolute maximum capacity, noted K_L^P, which may never be exceeded. The control of RANKL concentration on the cell surface is represented by the following expression:

$$p_L - d_L = r_L \cdot \left(1 - \frac{L + O\bullet L + K\bullet L}{K_L^P \cdot \pi_P \cdot B}\right) + I_L, \tag{5}$$

where r_L is the rate of RANKL production and elimination, and I_L is a rate of external injection of RANKL. $L + O\bullet L + K\bullet L$ is the current total concentration of RANKL (free and bound), whereas the denominator corresponds to the imposed carrying capacity. In Eq. (5), the concentration of RANKL that the osteoblasts aim to produce is governed by the value of $\pi_P : K_L^P \cdot \pi_P \cdot B$. If the total concentration of RANKL $L + O\bullet L + K\bullet L$ is below this value to be reached, then the rate of production of RANKL is positive, otherwise it is negative. Pseudo steady states of the RANKL and OPG concentrations are calculated from Eqs. (3)–(5):

$$L = \frac{K_L^P \cdot \pi_P \cdot B}{1 + k_3 K/k_4 + k_1 O/k_2} \cdot \left(1 + \frac{I_L}{r_L}\right)$$

and

$$O = \frac{K_O^P}{k_O \pi_P} R + \frac{I_O}{k_O}.$$

The equations governing the evolution of the number of cells in each population are simply balance equations. Each compartment of cells is fed by an entering flow of fresh cells and is emptied by the outgoing flow of differentiated or apoptotic cells.

The osteoblast lineage is supplied from a large population of uncommitted progenitors. These progenitors express a specific TGF-β receptor which, once

activated, leads to the differentiation of the progenitors into ROBs. We suppose that the rate of release of TGF-β per active osteoclast is constant. Moreover, the binding kinetics of TGF-β with its receptor is faster than changes in AOC numbers. Thus, at any time, the concentration of TGF-β is proportional to the concentration of the AOCs. From this "fast" kinetics, it is a reasonable assumption to not include a TGF-β compartment. The TGF-β-induced effects on the progenitors are mediated by the active osteoclasts. The entering flow into the ROB compartment depends on the progenitors response to TGF-β binding. This response is represented by a proportionality relationship with the TGF-β receptor occupancy, π_C:

$$D_R \cdot \pi_C = D_R \cdot \frac{C + C^0}{C + C^s}, \tag{6}$$

D_R being a proportionality factor. C is the concentration of the AOCs, C^s corresponds to the dissociation binding coefficient of TGF-β with its receptor, and C^0 represents the basal concentration of the AOCs in the system. We note $C^0 = f_0 \cdot C^s$, where f_0 is a fixed proportion.

The outgoing flow of the ROB compartment is also the feeding flow to the AOB compartment. This time, TGF-β binding acts by inhibiting the differentiation of the ROBs resulting in a cell response inversely proportional to the TGF-β receptor occupancy, π_C:

$$\frac{D_B}{\pi_C} \cdot R = D_B \cdot \frac{C + C^s}{C + C^0} \cdot R.$$

D_B is a factor of proportionality. d_B is defined by the relation $D_B = f_0 \cdot d_B$, where f_0 is the fixed proportion defined above. Contrary to the osteoprogenitors, the ROBs are present in "finite" quantities. Thus the ROB differentiation rate depends on the concentration of the ROBs in the compartment.

Apoptosis is most often the final stage of the AOBs' life. However, some will become lining cells, or osteocytes. The rate at which the AOBs enter an apoptotic state is a first-order degradation process represented by $k_B \cdot B$.

RANK-RANKL binding promotes the differentiation of osteoclast precursors into active osteoclasts. The differentiation is proportional to the RANK occupancy ratio. This ratio is noted π_L, and is equal to $K \bullet L/K$ in the present case (see Eq. (A.2) in the appendix). The flow of differentiated precursors entering the AOC compartment is then given by

$$D_C \cdot \frac{K \bullet L}{K},$$

where D_C is the differentiation rate of the osteoclasts precursors.

TGF-β induces osteoclast apoptosis via binding to specific cell surface receptors (Siegel and Massague, 2003). This phenomenon may then be represented by a relation similar to expression (6)

$$D_A \cdot \pi_C \cdot C = D_A \cdot \frac{C + C^0}{C + C^s} \cdot C,$$

where D_A is a proportionality constant.

The average rate of new bone formed per unit of time per AOB, as well as the rate of bone resorbed per unit of time per AOC are not known experimentally, but have been calculated (Parfitt et al., 1996). The number of AOBs that it takes to form a unit quantity of bone as AOCs resorb in the same time is also not known. In addition, it is not known if the production of bone per AOB (as well as the resorption of bone per AOC) varies with time or with other aspects of the system. As a simple approximation, we consider that the rate of bone formation as well as the rate of bone resorption are constant during the timescale of the model. This hypothesis is based on histological evidences (Rodan, 1998). Thus, the total amount of bone formed or resorbed by the system depends primarily on the ratio of the AOCs to the AOBs, C/B. Since the parameter values of reference (see the appendix) were selected from normal bone that is neither gaining nor losing mass, then the resulting system is a state of reference. When the system is in its state of reference: $C/B = C_0/B_0 \approx 1.25$. Thus, the system has an overall catabolic action when $C/B > C_0/B_0$, whereas the system is anabolic when $C/B < C_0/B_0$.

A cursory examination of the parameters indicates three classes of parameters (for complete listing see the appendix). The first class corresponds to the physicochemical parameters k_1, k_2, k_O, k_3, k_4, k_5, k_6, k_P and r_L. These parameters generally remain fixed under different physiological conditions. They are also easily measured experimentally. The second class of parameters value may fluctuate slightly in the case the larger physiological environment changes. These are: C^s, k_B, D_R, f_0, d_B, D_C, D_A, K_O^P, K_L^P, S_P, and K. The last category corresponds to parameters: I_P, I_O and I_L. They are external parameters, directly under the control of the experimentalist. Some parameters, mostly the parameters of the first type, have values reported in the literature. The remainder of the parameters, as yet have not been determined experimentally. It is nonetheless possible to estimate a range of acceptable values for each parameter by checking the literature.

3. Model analysis and simulation results

Observable states in biological systems often correspond to stable states of the system. Generally in biology, these states are stationary states (i.e. homeostasis), or oscillating states (biological rhythms and homeorrhesis). Oscillating behaviors arise, as a rule,

after a steady state or its dynamical locale loses its stability. The dynamic behavior of the model can then be delineated by determining its steady states and their stability.

The stationary states of Eq. (A.1) (Appendix) are the roots of a fourth-order polynomial in three variables. An analytical solution consists of more than 200 terms, making it unusable in practice; we therefore solve for the roots numerically. The system admits only one fixed point in the local region of the parameter space. No bifurcation is detected in the region of the parameter space explored. The steady state is found to be stable, even for some extreme values of the parameters. We introduced time delays in the equations to simulate non-instantaneous cellular response by retarding the receptor occupancy functions π_C and π_L (i.e. $\pi_C(t-\tau_1)$ and $\pi_L(t-\tau_2)$). We were curious about the effect of the delays on the stability of the fixed point. The consequences of mild retardations on the system trajectories were slight, and the fixed point remained stable. The stability and bifurcation analysis of the retarded system was done by using DDE-BIFTOOL (Engelborghs et al., 2001). The steady state was destabilized through a Hopf bifurcation only when unrealistically large delays were used ($\tau_{1,2} > 50$ days). This outcome is reassuring and suggests that the regulation of the bone mass is both stable and robust (at least, the modeling we made of it).

To illustrate the tight correlation between osteoblast and osteoclast functions, we computationally perturbed the system by adding or removing cells from specific compartments. From the very stable nature of the steady state, we expect that the immediate consequence is a rapid attainment of a new equilibrium. The behavior of the other modeling cell types reveals the intriguing internal regulatory structure of the model. The results of these computational experiments are displayed in Fig. 2A, where, from top to bottom, AOBs, AOCs and ROBs are alternately added at a constant rate and in Fig. 2B, where the same types of cell are removed. All graphs in Fig. 2 present temporal cell concentrations. Shortly after the administration of AOBs (precisely, half a day later), we observe that the level of AOCs also increases, similar to what is observed experimentally. The ROBs react with an even stronger buffering to the administration of AOBs (more than two days later) also by growing in number.

The order in which AOCs and ROBs are affected after removal of AOBs is the same observed by the addition of AOBs (Fig. 2B). The responding osteoblasts are the first to respond after the delivery of AOCs, their population growing to an even higher steady state. The AOBs react shortly after and also reach a higher equilibrium, but only after a transient decrease due to the dual action of TGF-β on the osteoblastic lineage.

Administration or removal of AOCs exhibit more complex patterns. An example is shown in Fig. 2B (middle graphic), where a pronounced decrease in AOCs results in a marked decrease in ROBs and a simultaneous increase in AOBs. This response induces a distinct growth of AOCs, and so on, leading to a sequence of damped oscillations. A less known phenomenon takes place when ROBs are administered to the system. The active osteoblasts increase in number, but the active osteoclasts develop, after transients, to a practically identical equilibrium (Fig. 2A, bottom graphic). This surprising phenomenon is interesting because the elevated production of AOBs is not associated with a higher production of AOCs. This novel observation may have the potential to be exploited as a therapeutic target for metabolic bone disease. Inversely, the removal of ROBs induces a drop of AOBs, whereas the AOC population maintains again, after transients, at about the same level (Fig. 2B, bottom graphic). This unusual situation is observed experimentally during space flight and in models of microgravity or disuse osteopenia. Experimentally, it has been shown that a lowered proliferation of preosteoblasts, in turn causes a decrease in osteoblast recruitment (Barou et al., 1998), with unaltered osteoclast activity (Jee et al., 1983; Turner et al., 1995; Carmeliet et al., 2001).

The only systemic hormone included in the model is PTH. As mentioned earlier, continuous infusion of PTH has potent catabolic effects on bone mass (Dempster et al., 1993; Goltzman, 1999). To test the catabolic action of PTH in the model, the hormone is delivered at a steady rate of 1000 pM/day for 60 days (Fig. 2C, top graphic). Continuous PTH induces an elevation in AOCs, ROBs and AOBs, leading, as expected, to an appreciable bone loss. This simulation is identical to numerous experimental and clinical observations (Tam et al., 1982; Watson et al., 1999).

OPG biological effects include inhibition of proliferation, differentiation, survival, and fusion of osteoclastic precursor cells; inhibition of the activation of osteoclasts; and promotion of osteoclasts apoptosis in vitro (Hofbauer et al., 2001a). In the model, introduction of OPG leads to a rapid decrease in AOCs, as well as ROBs, and a less pronounced decrease in AOBs (Fig. 2C, middle graphic). The overall effects are a reduction in bone turnover (decline of the bone cells volume), and an increase in bone mass. These results corroborate experimental observations indicating that high OPG levels induce profound osteopetrosis (increase in bone density), coincident with a decrease in osteoclast differentiation (Simonet et al., 1997). However, we have not found any source documenting the consequences of high OPG levels on osteoblasts; thus no comparison with the model can be made on that point.

Similarly, observations have shown that administration of RANKL results in reduced bone volume,

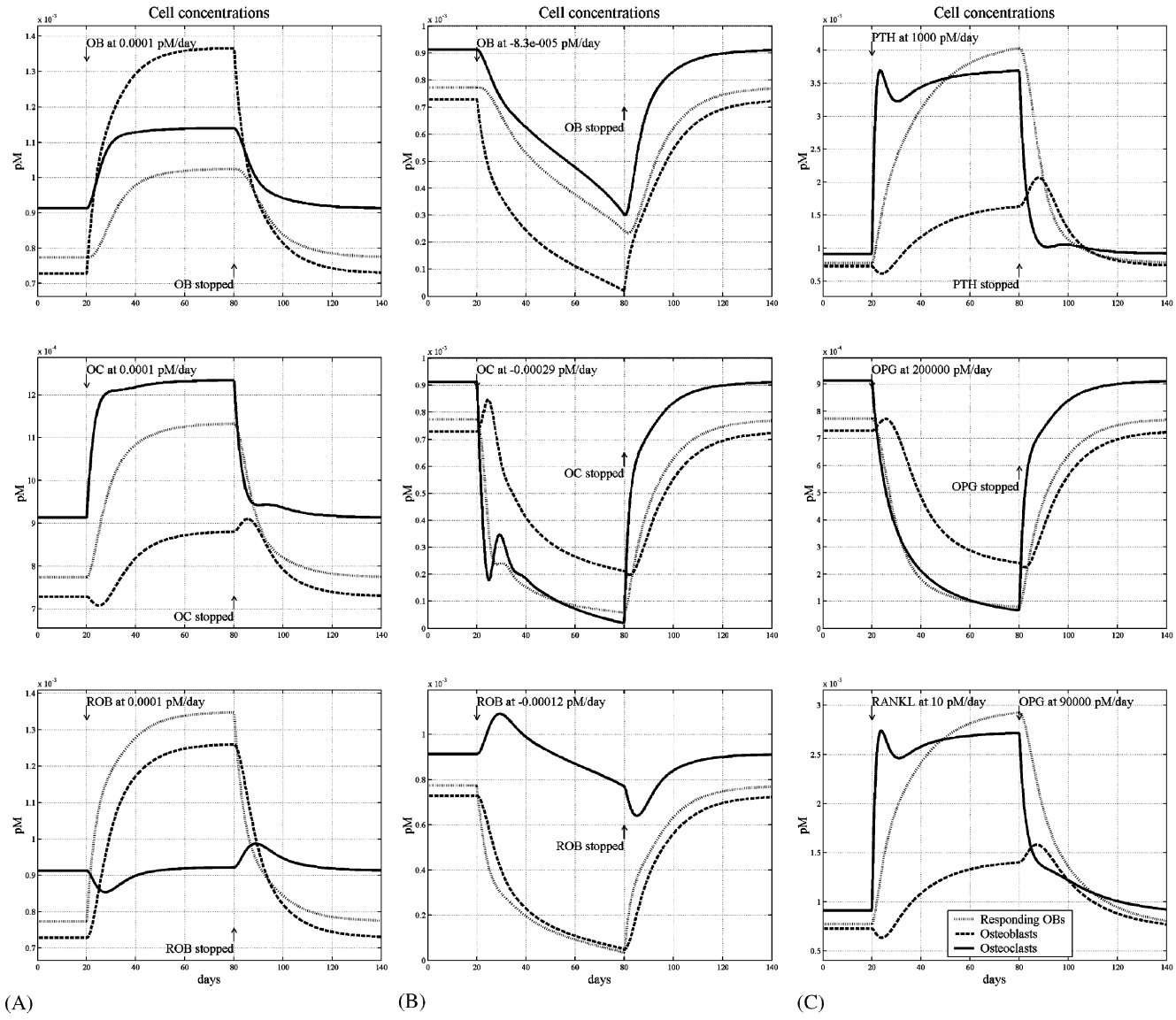

Fig. 2. In column A, we show the concentrations of the bone cells after adding ROBs, AOBs or AOCs, respectively, for 40 days at a constant rate. In column B, we show the same concentrations of the bone cells, but this time, after withdrawing ROBs, AOBs or AOCs, respectively, for 40 days at a constant rate. In column C, we show again the concentrations of the bone cells after injecting PTH or OPG, respectively, for 60 days at a constant rate (top and middle graphics). In the bottom graphic, we inject at a constant rate RANKL and, 60 days later, OPG. Solid curves, dashed curves, and dotted curves correspond, respectively, to temporal concentrations in OC, OB, and ROB.

increases osteoclast activity, and leads to a higher circulating concentration of calcium (Filvaroff and Derynck, 1998; Manolagas, 2000). Moreover, the effects of RANKL are reversed upon administration of OPG (Lacey et al., 1998). The antagonistic effects of RANKL and OPG are well simulated by the model (Fig. 2C, bottom graphic) and show excellent agreement with the known experimental data (Lacey et al., 1998). Indeed, the administration of RANKL increases the osteoclast population, while the osteoblasts grow only moderately (Fig. 2C, bottom graphic). In the presence of excess RANKL, normal bone cells numbers are restored by the injection of OPG (Fig. 2C, bottom graphic).

4. Discussion

It is apparent that RANK, RANKL and OPG form a fundamental cytokine system that is capable of influencing all aspects of osteoclast functions and, indirectly, the complete bone regulatory network (Aubin and Bonnelye, 2000). The balance between bone formation and bone resorption is regulated by the fluctuations of the local RANKL-to-OPG ratio. Sometimes this ratio may be chronically disturbed by local or systemic dysfunctions, giving rise to metabolic bone diseases (Manolagas, 2000). A number of cytokines, hormones and drugs have been shown to act primarily by

modulating the RANKL-to-OPG ratio (Hofbauer et al., 1998, 1999a,b, 2001b; Teitelbaum, 2000; Brandstrom et al., 2001; Chung et al., 2001; Sasaki et al., 2001; Viereck et al., 2002). The understanding of the central role played by the RANK-RANKL-OPG axis and, in particular, its interaction with the other components of the bone regulatory network, opens avenues for new therapeutic strategies.

4.1. Simulation of bone diseases

Estrogen deficiency is the principal cause of postmenopausal osteoporosis. Estrogen deficiency results in an acceleration of the rate of bone remodeling with a net increase in both osteoblastogenesis and osteoclastogenesis, as well as in the number of osteoblast progenitors (Manolagas, 2000). The consequences are a profound bone mineral loss. The action of estrogen seems to be mediated, at least in part, by OPG. Under normal conditions, estrogen stimulates the production of OPG; thus, in the case of estrogen deficiency, the concentration of OPG markedly decreases (Hofbauer et al., 1999b). As already mentioned, this disorder is rendered in the model by decreasing parameter K_O^P to 158 (normal value is 2×10^5). The new value of K_O^P is not chosen arbitrarily, it corresponds to the value that makes C/B increase from $C_0/B_0\approx1.25$ (normal ratio) to 5 (osteoporotic ratio). The ratio of 5 is our criterion for severe osteoporosis. Changes in the model solutions are shown in Table 1 and are in complete concordance with experimental observations.

PTH and the vitamin D hormone calcitriol ($1,25(OH)_2D_3$) are two major calcium regulating hormones (Feldman, 1999). Calcitriol controls parathyroid gland growth and, under normal range of activity, suppresses the synthesis and secretion of PTH (Slatopolsky et al., 1999); calcitriol decreases the number of PTH receptor number as well (Titus et al., 1991; Xie et al., 1996). In the case of $1,25(OH)_2D_3$ deficiency, PTH synthesis and PTH receptor production are no more inhibited, and increase. The effects of calcitriol deficiency are simulated in the model by setting the PTH synthesis rate S_P to 3765 pM/day. The consequences of this change are summarized in Table 1. For a number of reasons, the effects of vitamin D_3 deficiency on the bone cells have not been as clearly established as in the case of estrogen deficiency (Adelina and Fernandes, 2000) (this uncertainty is represented by the symbol '$\sim$' in Table 1). It is known that, depending on its release profile, PTH exhibits opposite effects on bone formation and resorption (Uzawa et al., 1995). Thus, depending on how the $1,25(OH)_2D_3$ deficiency is experimentally modeled in laboratories, the release pattern of PTH may be quite different from case to case. Moreover, it is currently under question that $1,25(OH)_2D_3$ may act directly on the osteoblastic lineage (van Leeuwen et al., 2001). However, in the case of continuous release of PTH, which actually corresponds to the way PTH is administered in the model, a net increase in bone resorption, bone turnover, osteoblasts and osteoclasts concentrations are observed (Kitazawa et al., 1991; Watson et al., 1999), in good correspondence with our simulation results.

The osteopenia associated with advanced age appears to be universal in humans and animals (Kahn et al., 1995). Although the mechanisms responsible are not completely understood, it seems that a decrease in the production of TGF-β is a critical step in disease

Table 1
Consequences of four major disorders of the bone regulatory system on the ratio C/B, the bone turnover and the bone cells concentrations

Cause: / **Consequence:**	Estrogen deficiency / Decreased OPG		$1,25(OH)_2D_3$ deficiency / Increased PTHr / PTH		Senescence / Decreased TGF-β		Glucocorticoid excess / Decreased ROB	
	Observed	Simulated	Observed	Simulated	Observed	Simulated	Observed	Simulated
C/B	↗	×4	~	×4	↗	×4	↗	×4
Bone turnover	↗	×10	↗	×10.2	~	×1.6	↘	÷1.6
AOB	↗	×3.8	↗	×3.8	↘	÷1.6	↘	÷4.3
AOC	↗	×15	↗	×15.3	~	×2.4	→	÷1.07
ROB	↗	×14.4	~	×14.5	↘	÷2.6	↘	÷4.5

The shaded columns designate disorders that generate an increased number of bone cells. For each type of disorder, the quantities showed in column one: C/B, the bone turnover ($C+B$), and the bone cells concentrations were measured experimentally (from different sources in the literature) and computed from the model. Naturally, up and down arrows indicate observations of, respectively, higher or lower quantities. Horizontal arrows indicate that no change in the measured quantity was observed. Experimental uncertainty is represented by the symbol '$\sim$'. Times and divide signs indicate how many times more (or less) each computed quantity was found to be in comparison to the steady state of reference.

progression (Nicolas et al., 1994; Kahn et al., 1995; Marie, 1997). We model this disorder by reducing the TGF-β content in bone by a factor of 5.5. The corresponding steady state is computed and shown in Table 1. The experimental observations in age-related osteoporosis have shown a reduction in both bone forming osteoblasts and osteoblastic stem cells. Other observations reveal either no change or an increase in both bone turnover and osteoclast numbers (Kahn et al., 1995; Marie, 1997). However, our simulations indicate an increase in both bone turnover and osteoclasts. This uncertainty may be associated with the difficulty of distinguishing the specific effects of senescence on bone remodeling from other causes of osteoporosis associated with old age (such as secondary hyperparathyroidism) (Riggs et al., 2002).

Glucocorticoid-induced osteoporosis (GIO) is another common cause of osteoporosis (Weinstein, 2001). GIO is characterized by a marked decrease in bone formation (Manolagas, 2000; Canalis and Giustina, 2001; Weinstein, 2001; Rubin and Bilezikian, 2002), a decrease in osteoblast progenitors (Weinstein, 2001), and a decrease in bone turnover (Rubin and Bilezikian, 2002). An early, transient increase in bone resorption is observed after initial exposure to glucocorticoids, followed by a slowing down (back-to-normal bone resorption) with uninterrupted use of glucocorticoids (Canalis and Giustina, 2001; Weinstein, 2001; Rubin and Bilezikian, 2002). Another common finding in GIO is a profound depression of bone formation (Manolagas, 2000; Weinstein, 2001; Rubin and Bilezikian, 2002). Exposure to glucocorticoids induces a decrease in the core binding factor A1 (Cbfa1) (Chang et al., 1998; Manolagas, 2000; Weinstein, 2001). Cbfa1 is an important osteoblastic differentiation factor (Ducy et al., 2000; Alliston et al., 2001), as its absence results in a complete block in osteoblastic differentiation and bone formation (Komori et al., 1997). In the model, glucocorticoid excess is simulated by decreasing D_R to 1.7×10^{-4} pM/day. Model simulations of this case are presented in Table 1, where it can be seen that they coincide in all aspects with experimental and clinical observations characterizing GIO. The concordance with the characteristics of GIO are highlighted by the model's prediction of a transient increase in osteoclasts, as shown in Fig. 2B (bottom graphic).

4.2. Therapeutic strategies

The model reliably simulates the normal bone regulation and the development of metabolic bone diseases and thus, may be useful in the development of new therapies that target restoration of bone turnover. For example, postmenopausal osteoporosis induced by estrogen deficiency is associated with a lack of production of OPG (Hofbauer et al., 1999b). In the model, estrogen-induced osteoporosis is simulated by decreasing the secretion rate of OPG by osteoblasts (K_O^P). It is then possible to systematically explore vast combinations of operations (i.e. variations of the model's parameters) that may restore normal bone turnover, for not net loss of bone. In the case of estrogen-induced osteoporosis, we can imagine a therapy that protects osteoblasts from apoptosis by decreasing the rate of elimination of AOB (represented by parameter k_B in the model). We hypothesize that this intervention would have a positive impact on bone formation; but is it really the case? Bone remodeling is extremely complex, the coupling between osteoblasts and osteoclasts may produce non-intuitive behaviors that modeling may reveal or predict.

There are two broad categories of therapy for osteoporosis. Anti-resorptive therapy depends exclusively on controlling osteoclasts, aiming for a net decrease in bone resorption (Rodan and Martin, 2000). There are sound practical reasons for expecting only moderate or minimal results from such treatment, since anti-resorptive therapy does not replace the compromised trabecular connectivity (Mosekilde and Reeve, 1996). Moreover Manolagas (Manolagas, 2000) defines anti-resorptive therapies as primarily, anti-remodeling since these therapies slow down the rate of bone remodeling, eventually leading to less bone apposition than fundamentally anabolic therapies.

The other category of therapy, bone formation therapy, aims to increase bone formation. The classic anabolic therapy is the pulsatile administration of PTH, which has been shown to yield net bone formation (Dempster et al., 1993). In principle, an ideal therapy for bone loss, especially in postmenopausal osteoporosis, would be to drive the bone resorption-to-formation ratio in favor of bone apposition (i.e. $C/B\approx1$). Such an intervention will allow the patient to regain lost bone mass and to maintain that bone gain. Such therapy would ideally achieve a bone turnover rate (i.e. the volume of active bone cells: C+B, also called rate of bone remodeling) 2–3 times higher than normal. In our case a normal bone turnover is $C+B=0.0016$ pM (when all parameters are set to their value of reference). Thus, the therapeutic value of bone turnover ranges approximately from 0.003 to 0.005 pM. A bone turnover rate lower than optimal would effectively lead to a slow bone apposition rate, that is not compatible with fast recovery. An increase in bone turnover beyond optimal may generate a large amount of insufficiently mineralized bone, with an erratic or uncontrolled apposition pattern and architecture.

Using our model, we examined four major dysfunctions of the bone regulatory system associated with a pathological bone resorption profile. Based on the criteria described in detail above, virtual therapies supporting a restoration of lost bone mass were

identified. The results of these investigations are presented in Table 2.

In Figs. 3–7, we illustrate different therapeutic attempts against the same bone diseases. In all figures, the graphs on the left display the ratio C/B as one parameter is varied. The arrows indicate the variation of the parameter from an osteoporotic situation ($C/B \approx 5$) to a therapeutic value of the ratio $C/B \approx 1$, which is indicated by a gray line. The value of reference $C/B \approx 1.25$ is indicated by a black line. The therapy is only acceptable if the bone turnover, displayed on the right graphs, stays within the therapeutic range defined earlier and indicated by a gray zone. Here also, the bone turnover value of reference $C + B = 0.0016\,\text{pM}$ is indicated by a black line.

Anti-resorptive therapies (see second half of Table 2) are never able to generate a bone turnover higher than normal, whereas a bone turnover slightly higher than normal is necessary for fast regain of bone loss (Mosekilde and Reeve, 1996; Manolagas, 2000). For instance, in the case of glucocorticoid excess, a therapy reducing the number of active osteoclasts, by increasing apoptosis (simulated in the model by increasing D_A to 36 day^{-1}), leads to over-suppression of bone turnover by a factor of 12 (as shown in Fig. 3). Conversely, bone formation therapies yield often better results as illustrated in Fig. 4. A therapy protecting active osteoblasts from apoptosis is applied in the case of glucocorticoid excess (in the model, this therapy consists in decreasing k_B to 0.026 day^{-1}). In this simulation bone turnover is doubled, which is consistent for a fast recovery of bone mass. The model indirectly suggests that pulsatile administration of PTH should be a good treatment for GIO. Indeed, pulsatile PTH may act to protect

Table 2
Effects of various therapeutic strategies against four major bone metabolic dysfunctions

Cause: / **Consequence:**	Estrogen deficiency / Decreased OPG	$1,25(OH)_2D_3$ deficiency / Increased PTHr / PTH	Senescence / Decreased TGF-β	Glucocorticoid excess / Decreased ROB
↗ D_R	High turnover ×47	High turnover ×16	High turnover ×3	n/s
↘ k_B	Unsuccessful	Unsuccessful	High turnover ×6	High turnover ×2
↗ f_0	Unsuccessful	Unsuccessful	High turnover ×2	Normal turnover
↘ C_s	Unsuccessful	Unsuccessful	Normal turnover	Low turnover ÷2
↘ d_B	Normal turnover	Normal turnover	Low turnover ÷3	Low turnover ÷12
↘ D_C	Normal turnover	Normal turnover	Low turnover ÷3	Low turnover ÷12
↗ D_A	Normal turnover	Normal turnover	Low turnover ÷3	Low turnover ÷12
↗ I_O	Normal turnover	Normal turnover	Low turnover ÷3	Low turnover ÷12
↘ K_L^P	Normal turnover	n/s	Low turnover ÷3	Low turnover ÷12
↗ K_O^P	n/s	Normal turnover	Low turnover ÷3	Low turnover ÷12
↗ K	Normal turnover	Normal turnover	Low turnover ÷3	Low turnover ÷12
Recommended Therapies:	↗ I_O + ↗ D_R	↗ I_O + ↗ D_R	↗ D_R or ↘ k_B + ↗ I_O	↘ k_B

Best therapies based on the model results are indicated (recommended therapies). The leftmost column contains model parameters whose variation (indicated by the arrow) tends to decrease the ratio C/B. The parameters in the shaded cells increase bone turnover when they are varied, whereas the others decrease bone turnover. Variations in these parameters represent potential therapeutic interventions. The five parameters above the double line separator correspond to bone formation therapies, the remainder of parameters correspond to anti-resorptive therapies. The four remaining columns display the degree of success of these therapies as simulated by the model. Using the same convention, the shaded cells designate disorders that generate an increased number of bone cells. The parameters of the first column are varied until the ratio C/B decreases to approximately 1. If the ratio C/B does not approach 1, the therapy is deemed ineffective and the mention 'unsuccessful' is written in the corresponding cell. If the ratio C/B is successfully decreased, the level of bone turnover achieved by the therapy is indicated (low, normal or high). The degree of increase (or decrease) in the rate of bone remodeling is mentioned. The mention 'n/s' means 'non-significant' and states that the parameter used to simulate the dysfunction is the same one that is used to simulate the therapy; the result is thus non-pertinent.

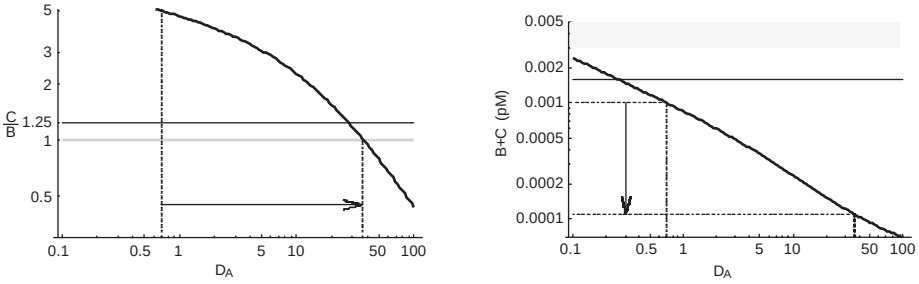

Fig. 3. Illustration of a bone anti-resorptive therapy by increasing osteoclasts apoptosis (increase in D_A) for correcting bone loss due an insufficient differentiation of osteoblastic progenitors (too low D_R) caused by glucocorticoid excess. In this case, the therapy induces a too low bone turnover (see right graph).

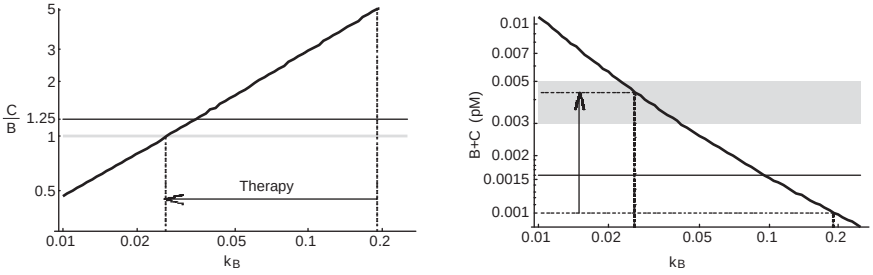

Fig. 4. Illustration of a bone formative therapy by protecting osteoblasts against apoptosis (decrease in k_B) for rebalancing bone loss due an insufficient differentiation of osteoblastic progenitors (too low D_R) caused by glucocorticoid excess.

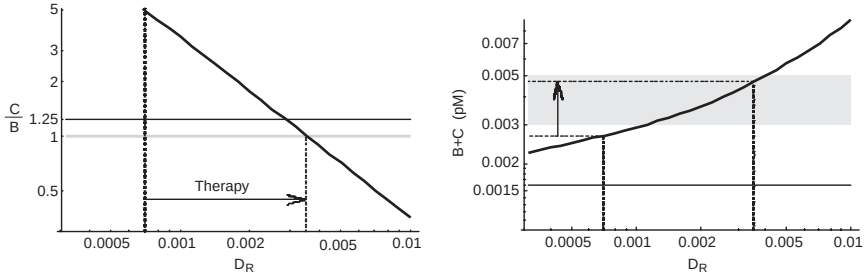

Fig. 5. Bone formative therapy by increasing the production of preosteoblasts (increase in D_R) to restore bone loss imbalance due to a reduced release of TGF-β caused by senescence.

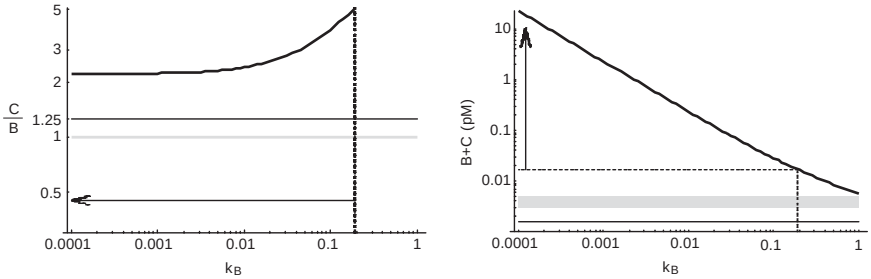

Fig. 6. Illustration of the failure (C/B too high) of a bone formative therapy (here, decrease in k_B) for equilibrating bone loss due an elevation of circulating PTH (too high S_P) caused by a deficiency in the vitamin D metabolism.

osteoblasts from apoptosis (Jilka et al., 1999). Such experimental paradigms are currently being evaluated.

Another example of a successful bone formation therapy is shown in Fig. 5. A therapy increasing the pool of differentiated osteoblastic progenitors (simulated in the model by increasing the parameter D_R to 3.5×10^{-3} pM/day) is applied to senescent bones. Although anabolic therapies are globally more successful than

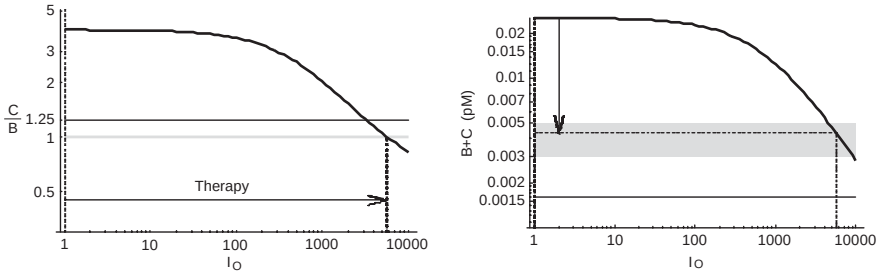

Fig. 7. An example of a dual therapy by increasing the proliferation of preosteoblasts (increase in D_R) in therapeutic combination with an injection of OPG. This therapy compensate for a bone loss due to a reduced production of OPG (too low K_O^P) caused by estrogen deficiency.

anti-resorptive therapies, some of them completely fail in restoring a normal ratio of bone resorption to bone formation, such as in the case of estrogen deficiency or $1,25(OH)_2D_3$ deficiency. This situation is illustrated in Fig. 6, where a reduction in osteoblast apoptosis (decrease in k_B) is unable to sufficiently reduce the ratio C/B, in the case of $1,25(OH)_2D_3$ deficiency. However this approach was a successful therapy in the case of GIO.

The model also predicts that no therapy is particularly efficacious against estrogen deficiency or $1,25(OH)_2D_3$ deficiency. Predicted therapies are either unsuccessful, or generate too high or, insufficient turnover values (see Table 2). One can think that an appropriate association between a therapy generating a high bone turnover with a therapy generating an insufficient bone turnover could result in a therapy producing a bone turnover just inside the therapeutic range. We thus tried a combination therapy by associating an anti-resorptive therapy (injection of OPG at 5623 pM/day) with an anabolic therapy (increase in D_R to 1.2×10^{-3} pM/day). The results of this dual therapy are shown in Fig. 7, and indicate an adequate bone turnover, 2.6 times higher than normal. Combinations of anabolic therapies with anti-resorptive agents have already been tested experimentally (Finkelstein, 1996; Mosekilde and Reeve, 1996), and result, most of the time, in greater effects on bone turnover (Compston and Watts, 2002).

We remark that therapies based on parameters D_R, k_B and I_O distinguish from the others by their ease of handling in practice and their efficiency. For instance, increasing I_O is simply managed by an infusion of OPG. However, an increase in f_0 gives excellent results in the case of senescence, but f_0 is tightly associated with the modeling framework, so its practical existence is questionable. Based on these criteria, we indicated the most successful therapies in Table 2. We notice that almost all good therapies in Table 2 are built on an increase in parameter D_R, which then appears to be an essential ingredient of therapeutic bone regrowth.

5. Conclusion

In this paper, we propose a mathematical model of the interactions between osteoblastic and osteoclastic activities in bone remodeling. The model is based on the idea that the relative proportions of immature and mature osteoblasts control the degree of osteoclastic activity. Vice versa, the resorption of bone by osteoclasts releases cytokines in the local microenvironment which control the osteoblasts differentially depending on their stage of differentiation. Despite the tremendous complexity of the bone regulatory system and its fragmentary understanding, we are able to obtain good correlations between the model simulations and the experimental observations extracted from the literature. The model results corroborate all known behaviors of the bone remodeling system that we have simulated, including the tight coupling between osteoblasts and osteoclasts, the catabolic effect induced by continuous injection of PTH, the catabolic action of RANKL, and its reversal by OPG administration, as well as bone loss induced by unloading. The model was also able to simulate the development of metabolic diseases such as estrogen deficiency, calcitriol deficiency, senescence and glucocorticoid excess. Conversely, possible therapeutic interventions are tested and evaluated in silico. Our model confirms the clinical data that anti-resorptive therapies are unable to directly regain bone loss, whereas bone formation therapies produce significant increases in bone mass. The model provides a mechanism to evaluate potential therapies based on their efficiency and their ease of implementation. In particular, the model predicts that combinations of anti-resorptive with anabolic therapies may provide better results than monotherapy. Finally, the model clearly suggests that increasing the preosteoblastic population by increasing the differentiation of mesenchymal progenitors (or modulating apoptosis) is a novel target for the therapeutic stimulation of bone formation. This model was originally developed as the first step of a bone metabolism modeling platform. These results are

extremely encouraging and warrant further detailed exploration of the model and direct experimental evaluation.

Appendix. A

A.1. Model's assumptions

- Our model is based on the convergence principle as an effective control process. The concept of "convergence", appeared for the first time in a paper by Hofbauer (Hofbauer et al., 2000), stipulates that the activity of pro-resorptive and anti-resorptive agents (whatever they are local or systemic) "converges" at the level of OPG and RANKL, whose final ratio controls the degree of osteoclast differentiation, activation, and apoptosis (Aubin and Bonnelye, 2000).
- Bone remodeling is carried out by temporary anatomic structures, basic muticellular units (BMU), which excavate and fill in tunnels through cortical bone or trenches across the surface of cancellous bone (Frost, 1983). As the bone matrix is more or less homogeneous at the scale of a BMU, spatial effects are ignored. What is important to us is the amount of bone that is formed or removed by the cells in the BMUs.
- During remodeling, BMUs are activated, as well as a series of specific sequenced events (stimuli, signal transduction, osteoclast activation, bone resorption, and bone formation) (Parfitt et al., 1996; Rodan, 1996). In the model, this clear temporal ordering is ignored because the domain of the model is a population of BMUs distributed over a section of bone. Hence the variables of the model represent ensemble averages. However, the ordering in time of the remodeling events is not completely lost because the domain is not too large. The size of the domain is chosen so that the BMUs of the domain are under the influence of the same kind of external stimuli at any time.
- The mechanical triggering of bone remodeling is not the only determinant. Bone continues to remodel in environments where the level of mechanical stress is low or non-existent as in space or during in vitro experiments (Akamine et al., 1992; Ma et al., 1995). We think that the mechanism responsible for the detection and transmission of mechanical stimuli is not an intrinsic, foundational part of the coupling, it is not included in the model.
- The availability of the osteoblastic progenitors is considered unlimited in the model. The same applies for the osteoclastic precursors.
- The model does not strictly take into account individual differences in cell life span and cell vigor. Changes in active osteoblast and osteoclast numbers really represent changes in "global" cell activity (i.e. composite changes in cell numbers, life span or vigor).
- The type of osteoblastic cell producing RANKL has not been absolutely determined experimentally (Aubin and Bonnelye, 2000; Manolagas, 2000). In the model, we postulate that RANKL is essentially produced by active osteoblasts.
- It is not clearly known also which cell of the osteoblastic lineage produces OPG. We suppose that, in the model, OPG is secreted by the responding osteoblasts. This choice, as well as the choice of AOB as the RANKL expressing cells, amounts to saying that the relative proportions of immature and mature osteoblasts control, in the end, the degree of resorption. This idea was first mentioned by Thomas (Thomas et al., 2001), and seems to be supported by experimental findings.

A.2. Model's variables

The model variables and their initial value are listed below:

Symbol	Unit	Value of Reference	Description
R	pM	0.0007734	Responding osteoblasts
B	pM	0.0007282	Active osteoblasts
C	pM	0.0009127	Active osteoclasts

A.3. Model's equations

The model equations are summed up in this section. The equations of the cell interactions are the following:

$$\frac{dR}{dt} = D_R \cdot \pi_C - \frac{D_B}{\pi_C} \cdot R,$$
$$\frac{dB}{dt} = \frac{D_B}{\pi_C} \cdot R - k_B \cdot B,$$
$$\frac{dC}{dt} = D_C \cdot \pi_L - D_A \cdot \pi_C \cdot C, \quad \text{(A.1)}$$

where

$$D_B = f_0 \cdot d_B, \quad \pi_C = \frac{C + f_0 \cdot C^s}{C + C^s}$$
$$\text{and} \quad \pi_L = \frac{K \bullet L}{K}.$$

$K \bullet L$ is evaluated at equilibrium, since the binding reactions are much faster than the rest of the interactions in

the model, and we have

$$\frac{K \bullet L}{K} = \frac{k_3}{k_4} \cdot \frac{K_L^P \pi_P B}{1 + \frac{k_3 K}{k_4} + \frac{k_1}{k_2 k_O} \cdot \left(\frac{K_O^P}{\pi_P} R + I_O \right)} \cdot \left(1 + \frac{I_L}{r_L} \right), \tag{A.2}$$

where I_L and I_O are external injection of RANKL and OPG. π_P, the fraction of occupied PTH receptors, is given by

$$\pi_p = \frac{\bar{P} + P^0}{\bar{P} + P^s} \quad \text{with } \bar{P} = \frac{I_P}{k_P},$$

$$P^0 = \frac{S_P}{k_P} \text{ and } P^s = \frac{k_6}{k_5}.$$

A.4. Model's parameters

The model parameters, with their value and description, are listed below:

Symbol	Unit	Value	Description
C^s	pM	5×10^{-3}	Value of C to get half differentiation flux
D_A	day^{-1}	0.7	Rate of osteoclast apoptosis caused by TGF-β
d_B	day^{-1}	0.7	Differentiation rate of responding osteoblasts
D_C	pM day^{-1}	2.1×10^{-3}	Differentiation rate of osteoclast precursors
D_R	pM day^{-1}	7×10^{-4}	Differentiation rate of osteoblast progenitors
f_0	No dimension	0.05	Fixed proportion
I_L	pM day^{-1}	$0–10^6$	Rate of administration of RANKL
I_O	pM day^{-1}	$0–10^6$	Rate of administration of OPG
I_P	pM day^{-1}	$0–10^6$	Rate of administration of PTH
K	pM	10	Fixed concentration of RANK
k_1	$\text{pM}^{-1}\,\text{day}^{-1}$	10^{-2}	Rate of OPG-RANKL binding
k_2	day^{-1}	10	Rate of OPG-RANKL unbinding
k_3	$\text{pM}^{-1}\,\text{day}^{-1}$	5.8×10^{-4}	Rate of RANK-RANKL binding
k_4	day^{-1}	1.7×10^{-2}	Rate of RANK-RANKL unbinding
k_5	$\text{pM}^{-1}\,\text{day}^{-1}$	0.02	Rate of PTH binding with its receptor
k_6	day^{-1}	3	Rate of PTH unbinding
k_B	day^{-1}	0.189	Rate of elimination of active osteoblasts
K_L^P	pmol/pmol cells	3×10^6	Maximum number of RANKL attached on each cell surface
k_O	day^{-1}	0.35	Rate of elimination of OPG
K_O^P	pmol day^{-1}/pmol cells	2×10^5	Minimal rate of production of OPG per cell
k_P	day^{-1}	86	Rate of elimination of PTH
r_L	pM day^{-1}	10^3	Rate of RANKL production and elimination
S_P	pM day^{-1}	250	Rate of synthesis of systemic PTH

References

Adelina, C.M., Fernandes, M.H., 2000. Long-term effects of parathyroid hormone, 1,25-dihydroxyvitamin d(3), and dexamethasone on the cell growth and functional activity of human osteogenic alveolar bone cell cultures. Pharmacol. Res. 42 (4), 345–353.

Akamine, T., et al., 1992. Prostaglandin E2 prevents bone loss and adds extra bone to immobilized distal femoral metaphysis in female rats. Bone 13 (1), 11–22.

Alliston, T., Choy, L., et al., 2001. TGF-beta-induced repression of CBFA1 by Smad3 decreases cbfa1 and osteocalcin expression and inhibits osteoblast differentiation. Embo J. 20 (9), 2254–2272.

Aubin, J.E., 1998a. Advances in the osteoblast lineage. Biochem. Cell Biol. 76 (6), 899–910.

Aubin, J.E., 1998b. Bone stem cells. J. Cell. Biochem. 30–31 (Suppl), 73–82.

Aubin, J.E., Bonnelye, E., 2000. Osteoprotegerin and its ligand: a new paradigm for regulation of osteoclastogenesis and bone resorption. Medscape Womens Health 5 (2), 5.

Barou, O., Palle, S., et al., 1998. Hindlimb unloading in rat decreases preosteoblast proliferation assessed in vivo with BrdU incorporation. Am. J. Physiol. 274 (1 Pt 1), E108–114.

Bland, R., 2000. Steroid hormone receptor expression and action in bone. Clin. Sci. 98 (2), 217–240.

Bonewald, L.F., Dallas, S.L., 1994. Role of active and latent transforming growth factor beta in bone formation. J. Cell. Biochem. 55 (3), 350–357.

Boyce, B.F., Hughes, D.E., et al., 1999. Recent advances in bone biology provide insight into the pathogenesis of bone diseases. Lab. Invest. 79 (2), 83–94.

Brandstrom, H., Bjorkman, T., et al., 2001. Regulation of osteoprotegerin secretion from primary cultures of human bone marrow stromal cells. Biochem. Biophys. Res. Commun. 280 (3), 831–835.

Burgess, T.L., Qian, Y., et al., 1999. The ligand for osteoprotegerin (OPGL) directly activates mature osteoclasts. J. Cell Biol. 145 (3), 527–538.

Canalis, E., Giustina, A., 2001. Glucocorticoid-induced osteoporosis: summary of a workshop. J. Clin. Endocrinol. Metab. 86 (12), 5681–5685.

Carmeliet, G., Vico, L., et al., 2001. Space flight: a challenge for normal bone homeostasis. Crit. Rev. Eukaryot. Gene. Exp. 11 (1–3), 131–144.

Chang, D.J., Ji, C., et al., 1998. Reduction in transforming growth factor beta receptor I expression and transcription factor CBFa1 on bone cells by glucocorticoid. J. Biol. Chem. 273 (9), 4892–4896.

Cho, C., Greller, L., et al., 2000. Parathyroid hormone receptor and osteoporosis — towards target validation by mathematical modeling. King of Prussia, PA, USA, Bioinformatics Mathematical Biology, Bone & Cartilage Biology, SmithKline Beecham Pharmaceuticals R&D.

Chung, H., Kang, Y.S., et al., 2001. Deflazacort increases osteoclast formation in mouse bone marrow culture and the ratio of RANKL/OPG mRNA expression in marrow stromal cells. J. Korean. Med. Sci. 16 (6), 769–773.

Collin-Osdoby, P., Rothe, L., et al., 2001. Receptor activator of NF-kappa B and osteoprotegerin expression by human microvascular endothelial cells, regulation by inflammatory cytokines, and role in human osteoclastogenesis. J. Biol. Chem. 276 (23), 20659–20672.

Compston, J.E., Watts, N.B., 2002. Combination therapy for postmenopausal osteoporosis. Clin. Endocrinol. (Oxf) 56 (5), 565–569.

Dempster, D.W., Cosman, F., et al., 1993. Anabolic actions of parathyroid hormone on bone (published erratum appears in Endocr. Rev. 1994;15(2):261). Endocr. Rev. 14 (6), 690–709.

Du, P., Ye, Y., et al., 2000. Endogenous parathyroid hormone-related peptide enhances proliferation and inhibits differentiation in the osteoblast-like cell line ROS 17/2.8. Bone 26 (5), 429–436.

Ducy, P., Schinke, T., et al., 2000. The osteoblast: a sophisticated fibroblast under central surveillance. Science 289 (5484), 1501–1504.

Engelborghs, K., Luzyanina, T., et al., 2001. DDE-BIFTOOL: a Matlab package for bifurcation analysis of delay differential equations. Leuven, Belgium, Department of Computer Sciences, Free University.

Eriksen, E.F., Kassem, M., 1992. The cellular basis of bone remodeling. Triangle 31 (2/3), 45–57.

Feldman, D., 1999. Vitamin D, parathyroid hormone, and calcium: a complex regulatory network. Am. J. Med. 107 (6), 637–639.

Filvaroff, E., Derynck, R., 1998. Bone remodelling: a signalling system for osteoclast regulation. Curr. Biol. 8 (19), R679–R682.

Finkelstein, J.S., 1996. Pharmacological mechanisms of therapeutics: parathyroid hormone. Principles of Bone Biology, Academic Press, New York (Chapter 71) 993–1005.

Frost, H.M., 1983. The skeletal intermediary organization. Metab. Bone Dis. Relat. Res. 4 (5), 281–290.

Fujimori, A., Cheng, S.L., et al., 1991. Dissociation of second messenger activation by parathyroid hormone fragments in osteosarcoma cells. Endocrinology 128 (6), 3032–3039.

Goltzman, D., 1999. Interactions of PTH and PTHrP with the PTH/PTHrP receptor and with downstream signaling pathways: exceptions that provide the rules [editorial; comment]. J. Bone Mineral Res. 14 (2), 173–177.

Greenfield, E.M., Bi, Y., et al., 1999. Regulation of osteoclast activity. Life Sci. 65 (11), 1087–1102.

Gunther, T., Schinke, T., 2000. Mouse genetics have uncovered new paradigms in bone biology. Trends Endocrinol. Metab. 11 (5), 189–193.

Halladay, D.L., Miles, R.R., et al., 2001. Identification of signal transduction pathways and promoter sequences that mediate parathyroid hormone 1-38 inhibition of osteoprotegerin gene expression. J. Cell Biochem. 84 (1), 1–11.

Hauschka, P.V., 1989. Growth factors effects. In: Hall, B.K. (Ed.), Bone, Vol. 1. CRC Press, Boca Raton, FL, 512pp.

Hofbauer, L.C., Dunstan, C.R., et al., 1998. Osteoprotegerin production by human osteoblast lineage cells is stimulated by vitamin D, bone morphogenetic protein-2, and cytokines. Biochem. Biophys. Res. Commun. 250 (3), 776–781.

Hofbauer, L.C., Gori, F., et al., 1999a. Stimulation of osteoprotegerin ligand and inhibition of osteoprotegerin production by glucocorticoids in human osteoblastic lineage cells: potential paracrine mechanisms of glucocorticoid-induced osteoporosis [see comments]. Endocrinology 140 (10), 4382–4389.

Hofbauer, L.C., Khosla, S., et al., 1999b. Estrogen stimulates gene expression and protein production of osteoprotegerin in human osteoblastic cells. Endocrinology 140 (9), 4367–4370.

Hofbauer, L.C., Khosla, S., et al., 2000. The roles of osteoprotegerin and osteoprotegerin ligand in the paracrine regulation of bone resorption. J. Bone Mineral Res. 15 (1), 2–12.

Hofbauer, L.C., Neubauer, A., et al., 2001a. Receptor activator of nuclear factor-kappaB ligand and osteoprotegerin: potential implications for the pathogenesis and treatment of malignant bone diseases. Cancer 92 (3), 460–470.

Hofbauer, L.C., Shui, C., et al., 2001b. Effects of immunosuppressants on receptor activator of NF-kappaB ligand and osteoprotegerin production by human osteoblastic and coronary artery smooth muscle cells. Biochem. Biophys. Res. Commun. 280 (1), 334–339.

Huang, W.H., Zheng, M.H., 1999. Steroid hormones and bone. Histol. Histopathol. 14 (4), 1257–1268.

Isogai, Y., Akatsu, T., et al., 1996. Parathyroid hormone regulates osteoblast differentiation positively or negatively depending on the differentiation stages. J. Bone Mineral Res. 11 (10), 1384–1393.

Jee, W.S., Wronski, T.J., et al., 1983. Effects of spaceflight on trabecular bone in rats. Am. J. Physiol. 244 (3), R310–R314.

Jerome, C.P., Burr, D.B., et al., 2001. Treatment with human parathyroid hormone (1-34) for 18 months increases cancellous bone volume and improves trabecular architecture in ovariectomized cynomolgus monkeys (macaca fascicularis). Bone 28 (2), 150–159.

Jilka, R.L., Weinstein, R.S., et al., 1998. Osteoblast programmed cell death (apoptosis): modulation by growth factors and cytokines. J. Bone Mineral Res. 13 (5), 793–802.

Jilka, R.L., Weinstein, R.S., et al., 1999. Increased bone formation by prevention of osteoblast apoptosis with parathyroid hormone. J. Clin. Invest. 104 (4), 439–446.

Kahn, A., Gibbons, R., et al., 1995. Age-related bone loss. A hypothesis and initial assessment in mice. Clin. Orthop. (313) 69–75.

Kitazawa, R., Imai, Y., et al., 1991. Effects of continuous infusion of parathyroid hormone and parathyroid hormone-related peptide on rat bone in vivo: comparative study by histomorphometry. Bone Mineral 12 (3), 157–166.

Knauer, D.J., Wiley, H.S., et al., 1984. Relationship between epidermal growth factor receptor occupancy and mitogenic response. Quantitative analysis using a steady state model system. J. Biol. Chem. 259 (9), 5623–5631.

Komarova, S.V., Smith, R.J., et al., 2003. Mathematical model predicts a critical role for osteoclast autocrine regulation in the control of bone remodeling. Bone 33 (2), 206–215.

Komori, T., Yagi, H., et al., 1997. Targeted disruption of Cbfa1 results in a complete lack of bone formation owing to maturational arrest of osteoblasts. Cell 89 (5), 755–764.

Kroll, M.H., 2000. Parathyroid hormone temporal effects on bone formation and resorption. Bull. Math. Biol. 62 (1), 163–188.

Lacey, D.L., Timms, E., et al., 1998. Osteoprotegerin ligand is a cytokine that regulates osteoclast differentiation and activation. Cell 93 (2), 165–176.

Lauffenburger, D.A., Linderman, J.J., 1996. Receptors: Models for Binding, Trafficking, and Signaling. Oxford University Press, New York; Toronto.

Lowik, C.W., van Leeuwen, J.P., et al., 1985. A two-receptor model for the action of parathyroid hormone on osteoblasts: a role for intracellular free calcium and cAMP. Cell Calc. 6 (4), 311–326.

Ma, Y., et al., 1995. Partial maintenance of extra cancellous bone mass by antiresorptive agents after discontinuation of human parathyroid hormone (1–38) in right hindlimb immobilized rats. J. Bone Mineral Res. 10 (11), 1726–1734.

Ma, Y.L., Cain, R.L., et al., 2001. Catabolic effects of continuous human PTH (1–38) in vivo is associated with sustained stimulation of RANKL and inhibition of osteoprotegerin and gene-associated bone formation. Endocrinology 142 (9), 4047–4054.

Manolagas, S.C., 2000. Birth and death of bone cells: basic regulatory mechanisms and implications for the pathogenesis and treatment of osteoporosis. Endocr. Rev. 21 (2), 115–137.

Marie, P., 1997. Growth factors and bone formation in osteoporosis: roles for IGF-I and TGF-beta. Rev. Rhum. Engl. Ed. 64 (1), 44–53.

Martin, T.J., Ng, K.W., 1994. Mechanisms by which cells of the osteoblast lineage control osteoclast formation and activity. J. Cell. Biochem. 56 (3), 357–366.

Meng, X.W., Liang, X.G., et al., 1996. Temporal expression of the anabolic action of PTH in cancellous bone of ovariectomized rats. J. Bone Mineral Res. 11 (4), 421–429.

Mosekilde, L., Reeve, J., 1996. Treatment with PTH peptides. In: Marcus, R., Feldman, D., Kelsey, J. (Eds.), Osteoporosis. Academic Press, New York, pp. 1293–1311 (Chapter 68).

Mundy, G.R., 1999. Cellular and molecular regulation of bone turnover. Bone 24 (5 Suppl), 35S–38S.

Mundy, G.R., Boyce, B.F., et al., 1996. Cytokines and bone remodeling. In: Marcus, R., Feldman, D., Kelsey, J. (Eds.), Osteoporosis. Academic Press, New York, pp. 301–313 (Chapter 11).

Neer, R.M., Arnaud, C.D., et al., 2001. Effect of parathyroid hormone (1–34) on fractures and bone mineral density in postmenopausal women with osteoporosis. N. Engl. J. Med. 344 (19), 1434–1441.

Nicolas, V., Prewett, A., et al., 1994. Age-related decreases in insulin-like growth factor-I and transforming growth factor-beta in femoral cortical bone from both men and women: implications for bone loss with aging. J. Clin. Endocrinol. Metab. 78 (5), 1011–1016.

Parfitt, A.M., 1976. The actions of parathyroid hormone on bone: relation to bone remodeling and turnover, calcium homeostasis, and metabolic bone diseases. II. PTH and bone cells: bone turnover and plasma calcium regulation. Metabolism 25 (8), 909–955.

Parfitt, A.M., Mundy, G.R., et al., 1996. A new model for the regulation of bone resorption, with particular reference to the effects of bisphosphonates. J. Bone Mineral Res. 11 (2), 150–159.

Rattanakul, C., Lenbury, Y., et al., 2003. Modeling of bone formation and resorption mediated by parathyroid hormone: response to estrogen/PTH therapy. Biosystems 70 (1), 55–72.

Riggs, B.L., Khosla, S., et al., 2002. Sex steroids and the construction and conservation of the adult skeleton. Endocr. Rev. 23 (3), 279–302.

Rodan, G.A., 1996. Coupling of bone resorption and formation during bone remodeling. In: Marcus, R., Feldman, D., Kelsey, J. (Eds.), Osteoporosis. Academic Press, New York, pp. 289–299 (Chapter 10).

Rodan, G.A., 1998. Control of bone formation and resorption: biological and clinical perspective. J. Cell. Biochem. 30–31 (Suppl), 55–61.

Rodan, G.A., Martin, T.J., 1981. Role of osteoblasts in hormonal control of bone resorption—a hypothesis. Calc. Tissue Int. 33 (4), 349–351.

Rodan, G.A., Martin, T.J., 2000. Therapeutic approaches to bone diseases. Science 289 (5484), 1508–1514.

Roodman, G.D., 1999. Cell biology of the osteoclast. Exp. Hematol. 27 (8), 1229–1241.

Rubin, M.R., Bilezikian, J.P., 2002. Clinical review 151: the role of parathyroid hormone in the pathogenesis of glucocorticoid-induced osteoporosis: a re-examination of the evidence. J. Clin. Endocrinol. Metab. 87 (9), 4033–4041.

Sasaki, N., Kusano, E., et al., 2001. Glucocorticoid decreases circulating osteoprotegerin (OPG): possible mechanism for glucocorticoid induced osteoporosis. Nephrol. Dial. Transplant. 16 (3), 479–482.

Seeman, E., Delmas, P.D., 2001. Reconstructing the skeleton using intermittent parathyroid hormone. Trends Endocrinol. Metab.

Siegel, P.M., Massague, J., 2003. Cytostatic and apoptotic actions of TGF-beta in homeostasis and cancer. Nat. Rev. Cancer 3 (11), 807–821.

Simmons, D.J., Grynpas, M.D., 1990. Mechanisms of bone formation in vivo. In: Hall, B.K. (Ed.), Bone, Vol. I, A Treatrise. CRC Press, Boca Raton, FL.

Simonet, W.S., Lacey, D.L., et al., 1997. Osteoprotegerin: a novel secreted protein involved in the regulation of bone density. Cell 89 (2), 309–319.

Slatopolsky, E., Dusso, A., et al., 1999. New analogs of vitamin D3. Kidney Int. (Suppl.) 73, S46–S51.

Tam, C.S., Heersche, J.N., et al., 1982. Parathyroid hormone stimulates the bone apposition rate independently of its resorptive action: differential effects of intermittent and continuous administration. Endocrinology 110 (2), 506–512.

Teitelbaum, S.L., 2000. Bone resorption by osteoclasts. Science 289 (5484), 1504–1508.

Thomas, G.P., et al., 2001. Changing RANKL/OPG mRNA expression in differentiating murine primary osteoblasts. J. Endocrinol. 170 (2), 451–460.

Titus, L., Jackson, E., et al., 1991. 1,25-dihydroxyvitamin D reduces parathyroid hormone receptor number in ROS 17/2.8 cells and prevents the glucocorticoid-induced increase in these receptors: relationship to adenylate cyclase activation. J. Bone Mineral Res. 6 (6), 631–637.

Turner, R.T., Evans, G.L., et al., 1995. Spaceflight results in depressed cancellous bone formation in rat humeri. Aviat. Space Environ. Med. 66 (8), 770–774.

Uzawa, T., Hori, M., et al., 1995. Comparison of the effects of intermittent and continuous administration of human parathyroid hormone(1–34) on rat bone. Bone 16 (4), 477–484.

van Leeuwen, J.P., van Driel, M., et al., 2001. Vitamin D control of osteoblast function and bone extracellular matrix mineralization. Crit. Rev. Eukaryot. Gene. Expr. 11 (1–3), 199–226.

Viereck, V., Emons, G., et al., 2002. Bisphosphonates pamidronate and zoledronic acid stimulate osteoprotegerin production by primary human osteoblasts. Biochem. Biophys. Res. Commun. 291 (3), 680–686.

Watson, P.H., Fraher, L.J., et al., 1999. Enhanced osteoblast development after continuous infusion of hPTH(1–84) in the rat. Bone 24 (2), 89–94.

Weinstein, R.S., 2001. Glucocorticoid-induced osteoporosis. Rev. Endocr. Metab. Disord. 2 (1), 65–73.

Whitfield, J.F., Morley, P., et al., 2002. Bone growth stimulators. New tools for treating bone loss and mending fractures. Vitam. Horm. 65, 1–80.

Xie, L.Y., Leung, A., et al., 1996. Downregulation of the PTH/PTHrP receptor by vitamin D3 in the osteoblast-like ROS 17/2.8 cells. Am. J. Physiol. 270 (4 Pt 1), E654–E660.